J. Serb. Chem. Soc. 71 (6) 695–703 (2006)
JSCS-3463

UDC 669–03:539.24:655.226
Original scientific paper

Nanofabrication of planar split ring resonators for negative refractive index metamaterials in the infrared range

ZORAN JAKŠIĆ*, DANA VASILJEVIĆ-RADOVIĆ, MILAN MAKSIMOVIĆ, MILIJA SARAJLIĆ and ZORAN DJURIĆ

IHTM-Institut of Microelectronic Technologies and Single Crystals, Njegoševa 12, 11000 Belgrade, Serbia (e-mail: jaksa@nanosys.ihtm.bg.ac.yu)

(Received 25 May, revised 21 July 2005)

Abstract: Experimental nanofabrication of planar structures for one-dimensional metamaterials designed to achieve a negative effective refractive index in the mid-infrared range (5–10 micrometers) was performed. Double split ring and complementary double split ring resonators (SRR and CSRR) with square and circular geometries, were chosen to be fabricated since these are the basic building blocks to achieve a negative effective dielectric permittivity and magnetic permeability. Scanning probe nanolithography with *z*-scanner movement was used to fabricate straight-line and curvilinear segments with a line width of 80 – 120 nm. The geometries were delineated in 20 nm thin silver layers sputter-deposited on a positive photoresist substrate spin-coated on polished single crystal silicon wafers, as well as on polycarbonate slabs. The morphology of the structures was characterized by atomic force microscopy. The feature repeatibility was 60 – 150 nm, depending on the process conditions and the feature complexity. The nanolithographic groove depth in different samples ranged from 4 nm to 80 nm.

Keyeords: nanofabrication, scanning probe nanolithography, atomic force microscopy, metamaterials, negative refraction, split-ring resonators.

INTRODUCTION

Electromagnetic metamaterials with a negative refractive index (NRM)[1–6] may be defined as artificial subwavelength structures designed to simultaneously achieve negative values of the effective dielectric permitivity (ε) and the magnetic permeability (μ) in a given wavelength range, thus having a negative value of the effective refractive index. According to the *Science* magazine, NRMs were among the top ten scientific breakthrough of the year 2003.[7]

The direction of the Poynting vector in a negative index metamaterial is opposite to that of the wavevector, *i.e.*, the vectors of the electric and magnetic field, and the wavevector forms a left-oriented set. NRMs are, thus, sometimes called left-handed

* Corresponding author.

doi: 10.2298/JSC0606695J

metamaterials. Among the other names used for this specific type of artificial materials are double negative materials, backward media and Veselago media.

NRMs were first theoretically described by Veselago.[1] Independently of Veselago's work, Pendry rediscovered the same effect and proposed methods for its practical implementation.[2–4] The first experimental NRMs were realized in the experiments of Smith *et al.*[8,9]

There are many different phenomena peculiar to NRMs – reversal of the Snell law, the Doppler shift and the Čerenkov effect.[6] A number of novel applications were proposed using NRM. Probably the most important among them are "superlenses" or "perfect lenses",[10] which focus all Fourier components of a 2D image, including evanescent modes, thus furnishing resolutions beyond the diffraction limit. Another proposed application is as a subwavelength resonant structure,[11] *i.e.*, a resonator having dimensions much smaller than the operating wavelength.

Different practical solutions stemmed from these, *e.g.* high-gain, electrically small antennas for the microwave, materials possessing magnetic properties at THz frequencies, different microwave transmision lines,[11] directional couplers, resonators, filters, antireflection structures, as well as active optical elements based on nonlinear phenomena, *etc*.[12]

The first experimental building blocks acting as NRM included thin metalic wires[3] with a negative effective dielectric permittivity, and split ring resonators (SRR) for negative magnetic permeability.[4] The SRR (negative permeability elements, also described in literature as 'particles' or 'meta-atoms' of NRM[6], are arranged in unit cells, the multiplication of which furnishes a macroscopic NRM medium. Even though alternative methods have been proposed for the fabrication of NRM using the transmission line approach,[13–15] the SRR remains one of the basic building blocks used to achieve $\mu < 0$.

Different versions of single and double split rings were analyzed in a number of papers, their operating wavelengths ranging from the microwave to the infrared. Some of the proposed geometries are described in a recent article.[16]

In November 2004 *Phys. Rev. Lett*.[17] complementary split ring resonator structure was proposed. Such structures furnish a negative dielectric permittivity and thus are the first 'particle' alternative to thin wire and transmission line structures.

Since the dimensions of a NRM building block have to be strongly subwavelength, it is a difficult technological task to fabricate such structures for the optical range. The hitherto smallest experimental SRRs produced had features of about 5 μm, rendering a response in the infrared.[6] Some theoretical solutions to reach the near infrared wavelengths, and specifically a 1.55 μm operating wavelength have been described.[18]

In this paper, the fabrication of planar NRM ('metasurfaces') for the optical wavelength range using scanning probe nanolithography is analyzed. Different pla-

nar designs utilizing ordinary and complementary split ring structures and were analyzed and experiments were performed on their fabrication using our scanning probe nanolithographic system. The fabricated samples were characterized by atomic force microscopy (AFM).

THEORY

The basic building block of NRMs, the double split ring resonator (SRR), is a highly conductive ($\sigma \to \infty$) structure in which the capacitance between its two rings is large and balances its inductance. The essential operating principle of an SRR originates in its complex electromagnetic resonant capacitive and inductive response described by its equivalent L-C resonant circuit structure.[4] A time-varying magnetic field applied perpendicular to the surface of the rings induces currents which, in dependence on the electromagnetic resonant properties of the structure, produce a magnetic field that may either oppose or enhance the incident field, thus resulting in a positive or negative effective permeability. A complementary split ring (CSRR) is a complementary geometry to that of an SRR and, according to the Babinet principle, it is the unit cell of metamaterial/metasurfaces furnishing a negative ε.[17]

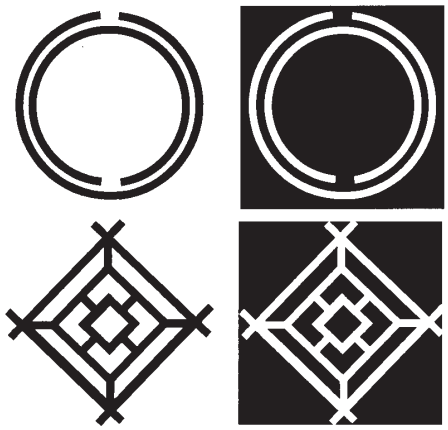

Fig. 1. Some double split ring geometries convenient for the optical range (shaded areas denote metal surface, white are nanolithographic 'cuts'). Top and bottom left: ordinary SRR; top and bottom right: complementary SRR. Top row utilizes circular and bottom row linear line segments.

Figure 1 shows the square and circular geometries chosen to consider for our design. The top left drawing shows the original SRR geometry with one capactive gap per ring, while the bottom left shows our geometries with several capacitive gaps. Circular geometries are shown in the top row, and linear in the bottom row. The right column shows the complementary structures.

The effective permeability and permittivity across a NRM unit cell are obtained as:

$$(\mu_{\text{eff}})_{x_i} = \frac{\langle B \rangle_{x_i}}{\mu_0 \langle H \rangle_{x_i}}, \qquad (\varepsilon_{\text{eff}})_{x_i} = \frac{\langle D \rangle_{x_i}}{\varepsilon_0 \langle E \rangle_{x_i}} \tag{1}$$

For the split ring resonator shown in Fig. 1 top left for the case when the rings

are in vacuum and their thickness is neglected, the following approximate expression is valid:[13]

$$\mu_{\text{eff}} = 1 - \frac{\pi r^2 / s}{1 + \dfrac{2\sigma i}{\omega\tau\mu_0} - \dfrac{3d}{\pi^2\mu_0\omega^2\varepsilon_0 r^3}} \tag{2}$$

where a is the unit cell length, d is the gap between the rings, and σ is the electrical conductance.

The resonant frequency (for which $\mu_{\text{eff}} \to \pm\infty$) is given by:

$$\omega_{0\text{m}} = \sqrt{\frac{3dc_0^2}{\pi^2 r^3}} \tag{3}$$

while the magnetic plasma frequency (for which $\mu_{\text{eff}} \to 0$) is given by:

$$\omega_{\text{pm}} = \sqrt{\frac{3dc_0^2}{\pi^2 r^3 (1 - \pi r^2 / a^2)}} \tag{4}$$

For a dielectric with ε and a ring line width w [19]:

$$\omega_{0\text{m}} = \sqrt{\frac{3dc_0^2}{\pi\varepsilon r^3 \ln(2w/d)}} \tag{5}$$

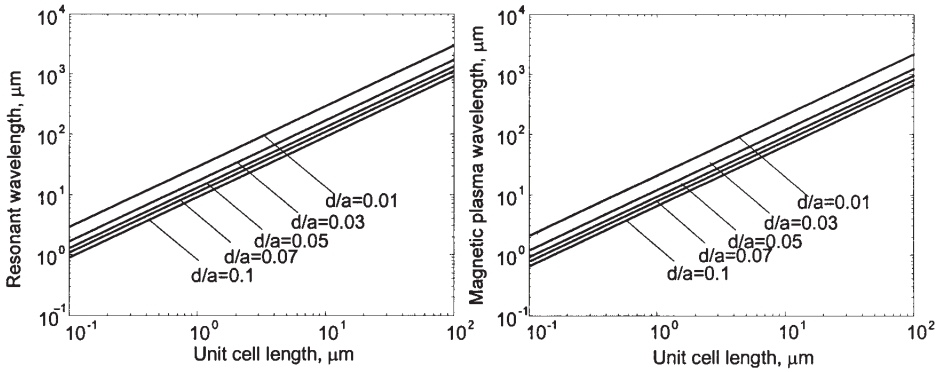

Fig. 2. The resonant (left) and magnetic plasma wavelength (rigt) for a range of unit cell dimensions of a circular double split ring resonator structure (Fig. 1. top left).

Based on Equations (2)–(5), the necessary unit cell dimensions to reach the optical wavelength range are readily calculated. For a circular split ring structure, a ratio of the unit cell to the SRR radius of 0.4 was chosen. The structure response for different inter–ring spacing values d were calculated. The results of the calculation of the plasma frequency are shown in Fig. 2, according to which, the unit cell dimensions must be 5 – 10 times smaller than the operating wavelength, depending on the chosen gap within the SRR. If nanolithographic lines of the order of 0.1 μm

are used (which defines the minimum gap between the rings), structures with minimum features 1.5 – 4 μm can be designed, thus the target wavelengths would be about 5 – 10 μm (mid-infrared).

According to the Babinet principle, *i.e.,* according to the duality and complementarity concepts, a CSRR structure exhibits an approximately dual behavior to that of the corresponding SRR.[17] This means that Equations (2)–(5), used to calculate the negative permeability of an SRR and its resonant frequency, can be used in a straightforward manner to approximately determine the effective permittivity and resonant frequency of a CSRR.[20] This was proven both theoretically[21] and experimentally.[20] Thus the whole consideration from the previous paragraph is applicable to the case of a CSRR by replacing μ_{eff} with ε_{eff}, while the resonant frequencies and ranges of negative permittivities of a CSRR remain identical to the case of the corresponding SRR.[20]

Another issue to be considered is the high frequency scalability of the forms described by Eqs. (2)–(4). The thickness of the metal layers for the SRR/CSRR must not be smaller than the skin depth (approx. 20 nm for silver at 100 THz).[18] Additionally, at wavelengths approaching the optical range, there is an additional inductance determining the plasma frequency, termed interial inductance, which is a consequence of the effective electron mass and the currents through an SRR being almost purely ballistic.[6] Thus for the scaled-down dimensions, the interial inductance becomes prevailing and the negative permeability/permittivity effect completely disappears. A method to overcome this problem has been proposed.[18] To this purpose, more capactive gaps were added to the original SRR design.

The bottom row of Fig. 1 (linear segments) shows double SRR and CSRR structures, where additional capactive gaps have been introduced to compensate fot the interial inductance. The geometries shown in the top row can be modified in the same manner.

The geometries shown in the bottom row represent our modification of the recently proposed ones[16,18] introduced with the aim of further decreasing the undesirable effects of intertial inductance.

EXPERIMENTAL

Sample preparation was commenced by using double polished silicon wafers. The wafers were spin-coated with a positive photoresist, 400 nm thickness and dried without baking. Further, RF sputtering was used to deposit a 20 nm thick silver layer over the photoresist. The surface morphology prior to nanolithography was characterized by atomic force microscopy. The flatness of the silver surface was better than 2 nm. Uncoated polycarbonate samples with a flatness of 10 – 30 nm were also used for the experiments.

The sample surfaces were nanolithographically processed to obtain NRM building blocks. To this purpose, scanning probe nanolithography using a Veeco Autoprobe CR-Research atomic force microscope (AFM) was employed.

The nanolithography process was performed under operating conditions standard for microelectronics/MEMS, *i.e.,* under normal atmospheric pressure and at room temperature and humidity.

However, antivibration and shock-free conditions were absolutely essential for proper operation. Such conditions were ensured by an anti-vibration table unit with active oscillation dumping. It is worth mentioning that even this sometimes failed to ensure disturbance-free operation and sometimes even any operation at all.

There are three modes of operation available on the Autoprobe CP-Research AFM: *z*-scanner movement ('scratching' mode), the voltage pulse mode (direct formation of oxide on the surface of silicon or other semiconductors) and the set-point nanolithography (the constant load mode). Of these three, the *z*-scanner movement mode was utilized.

A silicon nitride microcantilever tip was used for the operation. The scanner base position was adjusted to between 0.7 μm and 0.9 μm below the zero position, thus effectively pressing the needle tip against the sample surface with different forces of the order of nN. The real depth and width of the obtained nanolithographic lines depended on the aplied force, on the shape of the needle tip, the sample surface material and the speed of the needle tip (the slower the speed, the larger the depth).

RESULTS

Typical profiles of the fabricated nanolithographic lines are shown in Fig. 3.

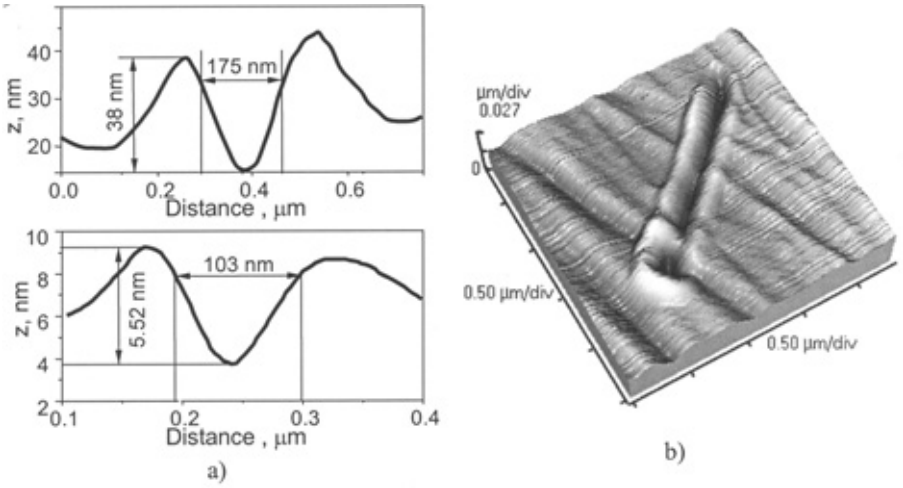

Fig. 3. Profiles and dimensions of nanolithographic lines, a) line profiles for a polycarbonate substrate (top) and silver on a photoresist (bottom); b) 3D AFM micrograph of a single nanolithographic line in polycarbonate.

It can be seen that the movement of the *z*-scanner nanolithography actually digs a groove in the substrate and leaves the 'upturned' material on its edges. This does not represent a problem with our structures of choice, since it is only important to physically disconnect thin metal surface while retaining the geometries its shown in Fig. 1.

The fabricated, straight-line (square) segment-based SRR structure is shown in Fig. 4. Each ring is split into four segments and the diagonal of the whole structure is 2.5 μm, while its inner square diagonal is about 1 μm. The *z*-scanner displacement was –0.7 μm and the nanolithographic line width was about 60 nm. Some lines in the obtained structure were displaced 60 – 150 nm from the designed values. Repeatability was tested by nanofabricating several identical structures and it also ranged between 60 and 150 nm.

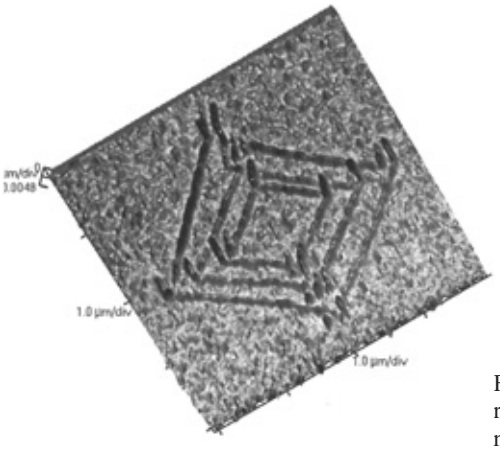

Fig. 4. AFM Profile of our square double split ring resonator structure fabricated by SPM nanolithography in silver on a photoresist.

Two complementary split ring structures with curvilinear segments, differing in the widths of their capacitive gaps, are shown in Fig. 5 (left and right). The outer diameter of the CSRRs was 2.2 μm, while the inner ring diameter was about 1 μm. The *z*-displacement here was larger (–0.9 μm), resulting in wider nanolithographic lines (about 80 nm).

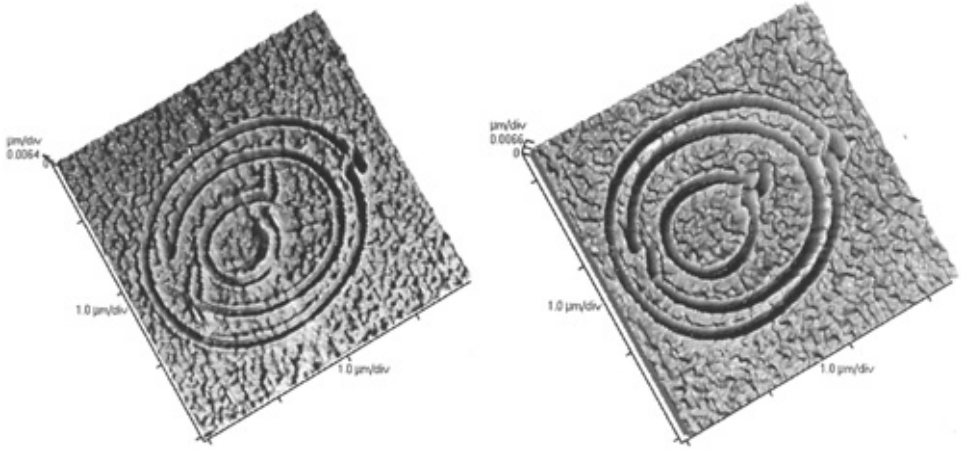

Fig. 5. AFM Profiles of two different double CSRR structures fabricated by SPM nanolithography in silver on a photoresist.

The duration of the process for a single SRR or CSRR was several seconds for straight-line segments, but it lasted 2–3 minutes for each curvilinear feature. The reason for the is that a circle is actually drawn as up to 360 linear segments. Additionally, each nanolithographic pattern requires full surface scanning before and after the process. Thus the fabrication of more complex patterns containing a larger number of elements ('particles') could be painstakingly slow.

Among the largest problems noted with the nanofabrication of the SRR and CSRR geometries was a gradual 'shifting' of the fabricated patterns compared to the

designed ones, most noticeable in a slight curving of the otherwise straight segments or in designed circles becoming spirals. An additional problem was that in some patterns a 'kink' at the beginning and at the end of each line appeared, 100 nm to 300 nm long, probably caused by the operation of the piezo-actuated micropositioner.

An advantageous property of the chosen silver substrates was that these were readily formed by the gallium nitride needle tip.

CONCLUSION

Basic double split ring and complementary double split ring resonator (SRR and CSRR) geometries for NRI materials in the optical wavelength range have been fabricated in 20 nm thick silver layers using *z*-scanner movement nanolithography. The obtained morphology of the samples was characterized by AFM. The best achieved resolution was 80 – 120 nm, and the feature repetability was 60 – 150 nm, depending on the process conditions and the feature complexity. The nanolithographic groove depth in different samples ranged from 4 nm to 80 nm.

Our further works should include fabrication of other alternative geometries and the production of larger 2D arrays of negative μ and ε particles, as well as the electromagnetic characterization of the thus obtained metasurfaces. This should include spectral transmission measurement by IR microscopy, as well as magnetic force microscopy measurements of the metasurfaces.

Acknowledgment: The authors wish to thank Ms. Mirjana Popović, BSCE and Ms. Kristina Blagojević, IHTM–IMTM for their preparation of the sample substrates. This work was partially funded by the Serbian Ministry of Science and Environmental Protection within the framework of the Project TR-6151B.

ИЗВОД

НАНОФАБРИКАЦИЈА ПЛАНАРНИХ СПЛИТ РИНГ РЕЗОНАТОРА ЗА МЕТАМАТЕРИЈАЛЕ СА НЕГАТИВНИМ ИНДЕКСОМ ПРЕЛАМАЊА У ИНФРАЦРВЕНОМ ОПСЕГУ

ЗОРАН ЈАКШИЋ, ДАНА ВАСИЉЕВИЋ-РАДОВИЋ, МИЛАН МАКСИМОВИЋ, МИЛИЈА САРАЈЛИЋ и ЗОРАН ЂУРИЋ

Институт за хемију, технологију и металургију – Центар за микроелектронске технологије и монокристале, Његошева 12, 11000 Београд

Вршена је експериментална нанофабрикација планарних структура за једнодимензионалне метаматеријале пројектоване да достигну негативну вредност ефективног индекса преламања у средњеталасном инфрацрвеном опсегу (5–10 микрометара). Направљени су двоструки сплит ринг и комплементарни сплит ринг резонатори (SRR и CSRR) са квадратном и кружном геометријом, пошто се они могу користити као основни градивни блокови за достизање негативне ефективне диелектричне пермитивности и магнетске пермеабилности. Коришћена је нанолитографија сканирајућом сондом у режиму *z*-помераја сканера да би се направили праволинијски и закривљени сегменти са ширином линије 80 – 120 nm. Геометрија је делинеирана у 20 nm дебелим слојевима сребра депонованим спатеровањем на подлогу од фоторезиста нанету спинером

на полиране плочице монокристала силицијума, као и на поликарбонатним плочицама. Морфологија структура карактрисана је "atomic force" микроскопом. Поновљивост детаља била је 60 – 150 nm, зависно од процесних услова и сложености детаља. Дубина нанолитографских бразди мењања је у опсегу од 4 do 80 nm.

(Примљено 25. маја, ревидирано 21. јула 2005)

REFERENCES

1. V. G. Veselago, *Sov. Phys. Uspekhi* **10** (1968) 509
2. J. B. Pendry, A. J. Holden, W. J. Stewart, I. Youngs, *Phys. Rev. Lett*. **76** (1996) 4773
3. J. B. Pendry, A. J. Holdenz, D. J. Robbins, W. J. Stewartz, *J. Phys. Cond. Matt.* **10** (1998) 4785
4. J. B. Pendry, A. J. Holden, D. J. Robbins, W. J. Stewart, *IEEE Trans. Microw. Theory Tech.* **47** (1999) 2075
5. J. B. Pendry, D. R. Smith, *Physics Today* **57** (2004) 37
6. S. A. Ramakrishna, *Rep. Prog. Phys.* **68** (2005) 449
7. Editorial, *Science* **302** (2003) 2039
8. D. R. Smith, W. J. Padilla, D. C. Vier, D. C. Nemal-Nasser, S. Schultz, *Phys. Rev. Lett*. **84** (2000) 4184
9. R. A. Shelby, D. R. Smith, S. Schultz, *Science* **292** (2001) 77
10. J. B. Pendry, *Phys. Rev. Lett.* **85** (2000) 3966
11. N. Enheta, *IEEE Ant. Wireless. Propag. Lett*. **1** (2002) 10
12. N. Engheta, Z. Zioklowski, *IEEE Trans. Microw. Theory Tech.* **53** (2005) 1535
13. G. V. Eleftheriades, A. K. Iyer, *IEEE Trans. Microw. Theory Tech.* **50** (2002) 2702
14. A. Grbić, G. V. Eleftheriades, *Journal of Applied Physics* **92** (2002) 5930
15. A. Grbić, G. V. Eleftheriades, *Phys. Rev. Lett*. **92** (2004) 117403
16. M. Kafesaki, Th. Koschny, R. S. Penciu, T. F. Goundogdu, E. N. Economou, C.M. Soukoulis, *J. Op. A: Pure Appl. Opt.* **7** (2005) S12
17. F. Falcone, T. Lopetegi, M. A. G. Laso, J. D. Baena, J. Bonache, M. Beruete, R. Marques, F. Martin, M. Sorolla, *Phys. Rev. Lett*. **93** (2004) 197401-1
18. S. O'Brien, D. McPeake, S. A. Ramakrishna, J. B. Pendry, *Phys. Rev. B*. **69** (2004) 241101
19. F. J. Rachford, D. L. Smith, P. F. Loschialpo, D. W. Forester, *Phys. Rev. E.* **66** (2002) 036613
20. F. Falcone, T. Lopetegi, J. D. Baena, R. Marqués, F. Martin, M. Sorolla, *IEEE Microw. Wireless Comp. Lett.* **14** (2004) 280
21. R. Marqués,J. D. Baena, M. Beruete, F. Falcone, T. Lopetegi, M. Sorolla, F. Martin, J. Garcia, *J. Opt. A: Pure Appl. Opt.* **7** (2005) S38.